

## Supporting information

Exploring the synergistic effect of alloying toward hydrogen evolution reaction: a case study of  $\text{Ni}_3M$  ( $M = \text{Ti}, \text{Ge}$  and  $\text{Sn}$ ) series

*Dong Zhang<sup>a</sup>, Shen-Jing Ji<sup>a</sup>, Yu Cao<sup>\*b</sup> and Nian-Tzu Suen<sup>\*a</sup>*

*a* College of Chemistry & Chemical Engineering, Yangzhou University, Yangzhou 225002, China

*b* College of Environmental Science and Engineering, Chemistry & Chemical Engineering, Yangzhou University, Yangzhou 225000, China

\*Corresponding author: Yu Cao ([yucao@yzu.edu.cn](mailto:yucao@yzu.edu.cn)), Nian-Tzu Suen ([006641@yzu.edu.cn](mailto:006641@yzu.edu.cn))

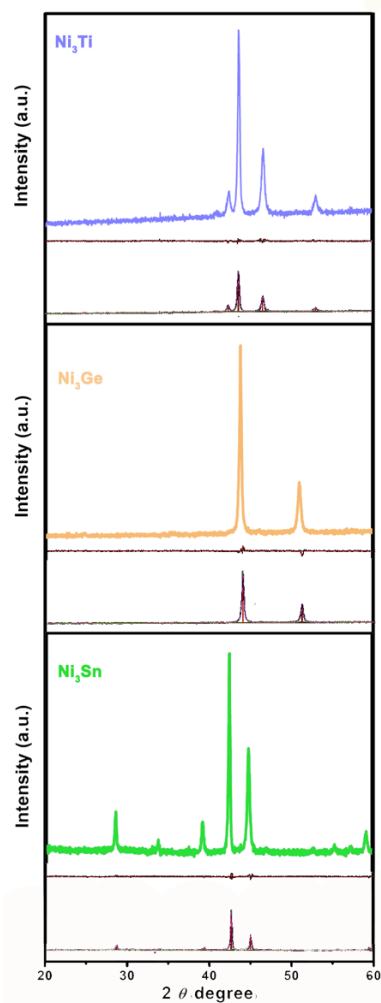


**Figure S1.** Experimental powder XRD patterns of  $\text{Ni}_3M$  ( $M = \text{Ti}, \text{Ge}$  and  $\text{Sn}$ ). The simulated pattern and difference between experimental pattern and simulated one was attached below. The refined lattice constants and interatomic distances were tabulated in Table S1.

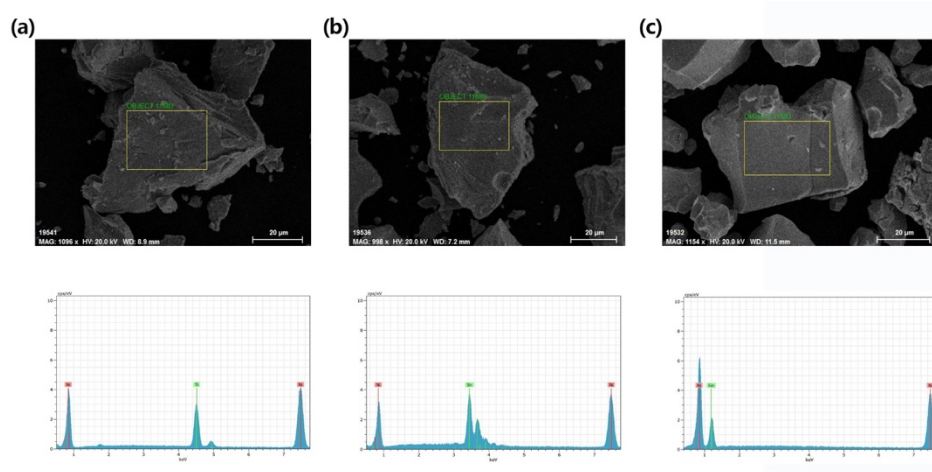


**Figure S2.** SEM image and EDX spectrum of  $\text{Ni}_3M$  ( $M = \text{Ti}, \text{Ge}$  and  $\text{Sn}$ ); (a)  $\text{Ni}_3\text{Ti}$ , (b)  $\text{Ni}_3\text{Ge}$  and (c)  $\text{Ni}_3\text{Sn}$ . The atomic ratio between Ni and  $M$  element of each sample derived from EDX analysis was shown in Table S2.

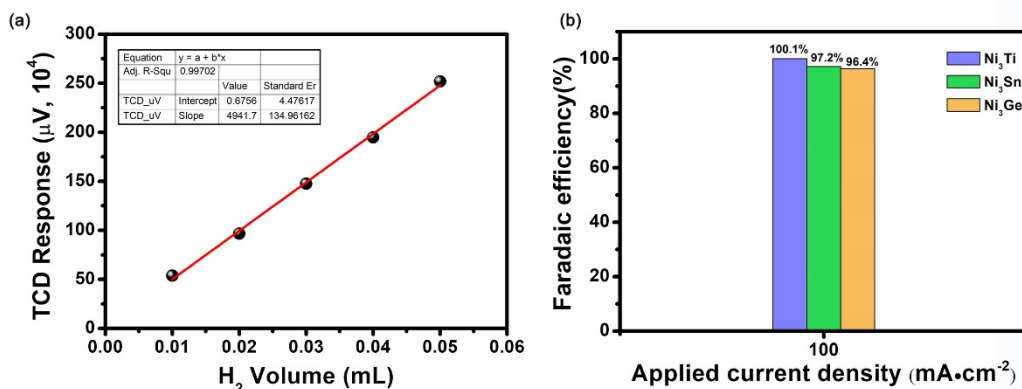


**Figure S3.** (a) H<sub>2</sub> Standard Line (b) applied current density-dependent Faraday efficiency (FE, %) curves of Hydrogen products of electrocatalytic for Ni<sub>3</sub>M ( $M = \text{Ti}, \text{Ge}$  and  $\text{Sn}$ ).

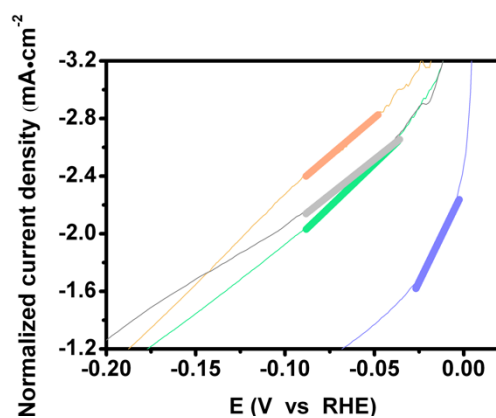


**Figure S4.** Tafel plots derived from normalized LSV based on roughness factor (RF) of Ni<sub>3</sub>M ( $M = \text{Ti}, \text{Ge}$  and  $\text{Sn}$ ) and Ni foam at 1.0 M KOH (scan rate:  $5 \text{ mV s}^{-1}$ ).

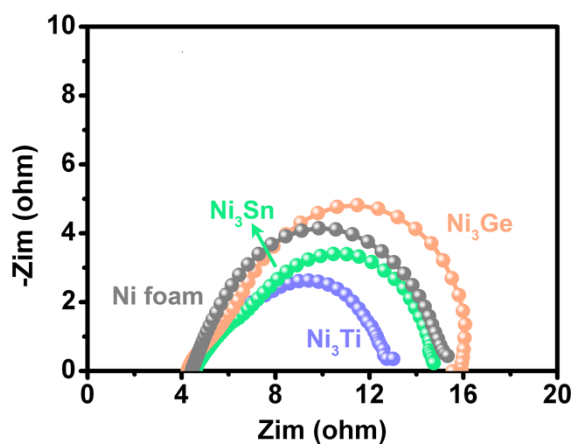


**Figure S5.** Electrochemical impedance spectroscopy (EIS) of Ni<sub>3</sub>M ( $M = \text{Ti}, \text{Ge}$  and  $\text{Sn}$ ) and Ni foam in 1.0 M KOH at -0.192 V (V vs RHE).

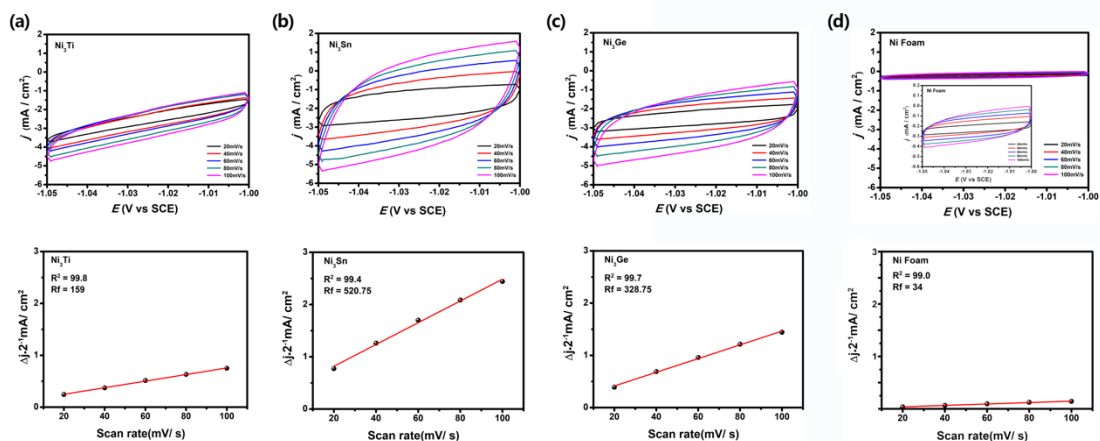


**Figure S6.** Cyclic voltammograms (CV) of  $\text{Ni}_3M$  ( $M = \text{Ti}, \text{Ge}$  and  $\text{Sn}$ ) in 1.0 M KOH; (a)  $\text{Ni}_3\text{Ti}$ , (b)  $\text{Ni}_3\text{Sn}$  (c)  $\text{Ni}_3\text{Ge}$  and (d) Ni Foam. Capacitive current density as a function of scan rate (20 – 100  $\text{mV s}^{-1}$ ). The derived roughness factor (RF) of each compound from the linear regression slope (specific capacitance  $40 \mu\text{F cm}^{-2}$ ) is included at bottom.

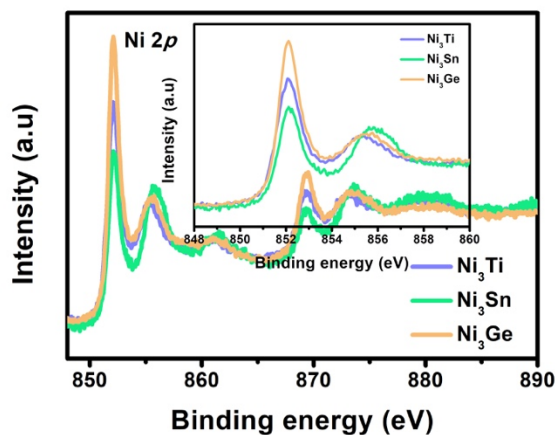


**Figure S7.** X-ray photoelectron spectrum (XPS) in the region of Ni 2p for  $\text{Ni}_3M$  ( $M = \text{Ti}, \text{Ge}$  and  $\text{Sn}$ ).

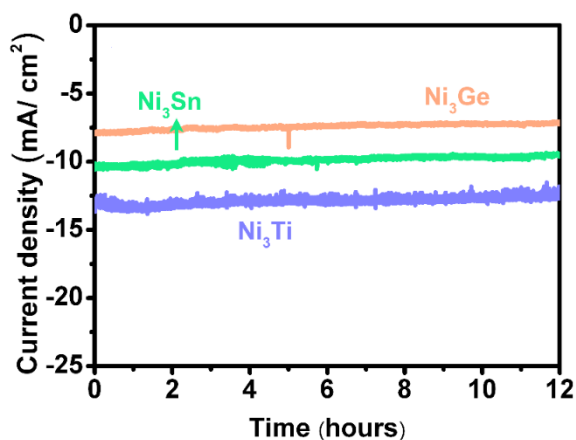


**Figure S8.** Chronoamperometry measurement of  $\text{Ni}_3M$  ( $M = \text{Ti}, \text{Sn}, \text{Ge}$ ) series over a period of 12 hours in 1.0 M KOH.

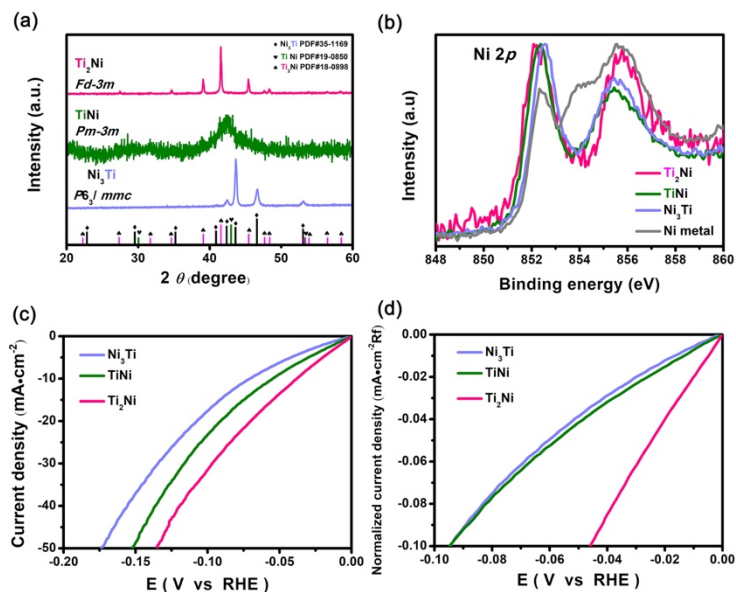


**Figure S9.** (a) Experimental powder X-ray diffraction (PXRD) patterns and (b) X-ray photoelectron spectrum (XPS) in the region of Ni 2p for  $\text{Ti}_2\text{Ni}$ ,  $\text{TiNi}$ , and  $\text{Ni}_3\text{Ti}$  (c) linear sweep voltammograms (LSV) and (d) normalized LSV based on roughness factor (RF) for  $\text{Ti}_2\text{Ni}$ ,  $\text{TiNi}$ , and  $\text{Ni}_3\text{Ti}$  at 1.0 M KOH (scan rate:  $5 \text{ mV s}^{-1}$ ).

**Table S1.** Refined lattice constants of  $\text{Ni}_3M$  ( $M = \text{Ti}, \text{Sn}, \text{Ge}$ ) series.

formula	lattice constants		averaged Ni–Ni bond distance ( $\text{\AA}$ )
	$a$	$c$	
$\text{Ni}_3\text{Ti}$	5.1017(1)	8.3076(1)	2.543
$\text{Ni}_3\text{Sn}$	5.288(1)	4.2416(1)	2.568
$\text{Ni}_3\text{Ge}$	3.5781(1)	3.5781(1)	2.530

**Table S2.** Atomic ratio of  $\text{Ni}_3M$  ( $M = \text{Ti}, \text{Ge}$  and  $\text{Sn}$ ).

Sample	Element	Atomic ratio (%)
$\text{Ni}_3\text{Ti}$	Ni	71.33
	Ti	28.67
$\text{Ni}_3\text{Ge}$	Ni	78.28
	Ge	21.72
$\text{Ni}_3\text{Sn}$	Ni	73.45
	Sn	26.55